

Photospheric Abundances of Volatile and Refractory Elements in Planet-Harboring Stars

Yoichi TAKEDA,¹ Bun'ei SATO,^{2,3} Eiji KAMBE,⁴ Wako AOKI,⁵
Satoshi HONDA,⁵ Satoshi KAWANOMOTO,⁵ Seiji MASUDA,⁶ Hideyuki IZUMIURA,²
Etsuji WATANABE,² Hisashi KOYANO,² Hideo MAEHARA,² Yuji NORIMOTO,²
Takafumi OKADA,² Yasuhiro SHIMIZU,² Fumihiro URAGUCHI,² Kenshi YANAGISAWA,²
Michitoshi YOSHIDA,² Shoken MIYAMA,⁵ and Hiroyasu ANDO⁷

¹*Komazawa University, Komazawa, Setagaya, Tokyo 154-8525*

takedayi@cc.nao.ac.jp

²*Okayama Astrophysical Observatory, National Astronomical Observatory,*

Kamogata, Okayama 719-0232

³*Department of Astronomy, School of Science,*

The University of Tokyo, Bunkyo-ku, Tokyo 113-0033

⁴*National Defence Academy, Yokosuka, Kanagawa 239-8686*

⁵*National Astronomical Observatory, Mitaka, Tokyo 181-8588*

⁶*Department of Astronomy, Faculty of Science, Kyoto University, Sakyo-ku, Kyoto 606-8502*

⁷*Subaru Telescope, National Astronomical Observatory of Japan,*

650 North A'ohoku Place, Hilo, HI 96720, U.S.A.

(Received ; accepted)

Abstract

By using the high-dispersion spectra of 14 bright planet-harboring stars (along with 4 reference stars) observed with the new coudé echelle spectrograph at Okayama Astrophysical Observatory, we investigated the abundances of volatile elements (C, N, O, S, Zn; low condensation temperature T_c) in order to examine whether these show any significant difference compared to the abundances of other refractory elements (Si, Ti, V, Fe, Co, Ni; high T_c) which are known to be generally overabundant in those stars with planets, since a T_c -dependence is expected if the cause of such a metal-richness is due to the accretion of solid planetesimals onto the host star. We found, however, that all elements we studied behave themselves quite similarly to Fe (i.e., $[X/Fe] \simeq 0$) even for the case of volatile elements, which may suggest that the enhanced metallicity in those planet-bearing stars is not so much an acquired character (by accretion of rocky material) as rather primordial.

Key words: stars: abundances — stars: atmospheres — stars: planet-harboring

1. Introduction

The topic of this paper concerns the chemistry of planet-harboring solar-type stars, which have recently been (and are now being) discovered one after another mostly by the Doppler technique thanks to the energetic activities of several groups.

It seems to have been almost established observationally that those stars bearing giant planets tend to be mildly metal-rich (i.e., $\sim+0.2$ dex on the average with a considerable scatter) compared to the Sun or similar standard stars, though there are some exceptions (see, e.g., Gonzalez et al. 2001; Sadakane et al. 2001, Santos et al. 2001; Smith et al. 2001; and references therein). What is now in hot debate is, however, the *cause* of this tendency — why does the existence of planets have something to do with the photospheric abundances of host stars?

Here, a promising and often invoked interpretation is the “self-enrichment” hypothesis. This attributes the origin of the overabundance of metals to the accretion of large amount of H-depleted (i.e., relatively metal-rich) rocky planetesimal materials onto the star, which is more or less reasonably understood from the viewpoint of the planet-formation process.

Following this line, theoretical as well as observational investigations have recently been done to clarify whether this mechanism accounts for the observed abundance characteristics also in the quantitative sense. Murray and Chaboyer (2001) arrived at a kind of affirmative conclusion that adding $\sim 6.5 M_{\oplus}$ of iron to each star can explain both the mass–metallicity and the age–metallicity relations of the stars with planets. Contrary to this, however, Pinsonneault et al. (2001) pointed out that an evident T_{eff} -dependence (i.e., more enhanced metallicity in earlier-type stars) must be observed if such an accretion mechanism is really responsible, which is not observed. Similarly, Santos et al. (2001) concluded by examining the shape of the metallicity distribution that the “pollution scenario” due to accretion is unlikely. They attributed the higher metallicity of planet-harboring stars to the simple fact that higher gas metallicity leads to the high probability of planet formation.

Meanwhile, another important key to check the “self-enrichment” hypothesis is to study the abundance pattern of various elements, especially the difference between the volatile elements (such as C, N, O) with low condensation temperature T_c (i.e., rather unlikely to be comprised in rocky materials) and the refractory elements (such as the iron-group elements) with high T_c (being apt to be condensed into solid particles). Namely, since the elements of the former group are expected to be deficient in the accreted materials relative to the latter, the abundances of the volatile group would not show such an overabundance as exhibited by the refractory group (e.g., Fe).

Then, is such a trend really observed? Sadakane et al.’s (1999) result for HD 217107, that C and O do not appear to share the tendency of marked overabundance shown by the other elements, may be suggestive for this prediction. Also, Gonzales and Laws (2000) once

stated that planet-harboring stars with $[\text{Fe}/\text{H}] > 0$ tend to be $[\text{C}/\text{Fe}] < 0$, again suggesting that C does not keep pace with the enrichment of Fe (though other stars without planets appear to show the similar tendency; see also Santos et al. 2000). Later, however, Gonzalez et al. (2001) withdrew this claim by stating “that stars with planets have low $[\text{C}/\text{Fe}]$ is found to be spurious, due to unrecognized systematic differences among published studies”. On the other hand, Smith et al. (2001) found that a small subset of planet-harboring stars (i.e., those with large planets orbiting quite close) exhibit a trend of increasing $[\text{X}/\text{H}]$ with an increase in T_c , which is a sign of the accretion of chemically fractionated solid material.

Thus, the situation is rather confusing, and a new systematic observational study is required to settle this problem. Following this motivation, we decided to investigate, based on our own observational data of bright planet-bearing stars collected at Okayama Astrophysical Observatory, whether any difference or systematic tendency exists between the abundances of volatile and refractory elements, which can be an important touchstone for the adequacy of the “self-pollution” scenario. This is the purpose of the present study, in which we will focus on the abundances of five volatile elements (C, N, O, S, and Zn) and compare them with those of the refractory elements (Si, Ti, V, Fe, Co, and Ni)

2. Observational Data

We observed 18 stars (14 planet-harboring stars and 4 reference stars) listed in table 1 by using the new high dispersion echelle spectrograph (HIDES; cf. Izumiura 1999) at the coudé focus of the 188 cm reflector of Okayama Astrophysical Observatory in 2000 April, 2000 October, 2000 December, 2001 February, and 2001 March.

The slit width was set to $200 \mu\text{m}$ ($0.''76$), by which the spectral resolution of $R \sim 70000$ was accomplished. By using the single $4\text{K} \times 2\text{K}$ CCD ($13.5 \mu\text{m}$ pixel), the wavelength span of $\sim 1200 \text{Å}$ could be covered at one time. We have chosen three wavelength regions: green-centered region ($4900\text{--}6100 \text{Å}$; G), red-centered region ($5900\text{--}7100 \text{Å}$; R), and (near-)IR-centered region ($7600\text{--}8800 \text{Å}$; I). All stars could be observed at both of the wavelength regions G and R, while the region I data could not be obtained for six stars (ϵ Eri, 51 Peg, HD 217107, 14 Her, τ Cet, and β Vir).

The reduction of echelle data (bias subtraction, flat-fielding, scattered-light subtraction, spectrum extraction, and wavelength calibration) was performed by using the IRAF¹ software package in a standard manner.

The S/N ratios of the resulting spectra differ from case to case, but are typically of the order of 200–300. However, the near-IR spectra turned out to be generally of poorer quality because interference fringes could not completely be removed.

¹ IRAF is distributed by the National Optical Astronomy Observatories, which is operated by the Association of Universities for Research in Astronomy, Inc. under cooperative agreement with the National Science Foundation.

Regarding the solar spectrum used as a reference standard, we adopted the very high resolution and very high S/N solar flux spectrum published by Kurucz et al. (1984).

3. Abundance Analysis

3.1. Model Atmospheres

With regard to the atmospheric parameters (T_{eff} , $\log g$, $[\text{Fe}/\text{H}]$, and ξ) of the program stars necessary for constructing model atmospheres and determining abundances, various published studies were consulted. We compared the published values from several sources (e.g., Gonzalez 1998; Gonzalez et al. 2001; Gonzalez, Law 2001; Fuhrmann 1998) for a same star when available, and found that they are generally consistent with each other and that the differences are in most cases within $\Delta T_{\text{eff}} \sim 100$ K and $\Delta \log g \sim 0.1$. The adopted parameter values (with the references) are presented in table 1.

We interpolated Kurucz’s (1993) grid of ATLAS9 model atmospheres in terms of T_{eff} , $\log g$, and $[\text{Fe}/\text{H}]$ to generate the atmospheric model for each star.

3.2. Determination of the Abundances

3.2.1. Equivalent width analysis

Regarding the target volatile elements (C, N, O, S, and Zn), as far as the lines of interest are neither blended nor too weak, we determined the abundances from the equivalent widths by using the WIDTH9 program, a companion program to the ATLAS9 model atmosphere program written by Dr. R. L. Kurucz (Kurucz 1993). As for the data of spectral lines (wavelengths, gf values, and damping parameters), we exclusively invoked the compilation of Kurucz and Bell (1995). The gf values of important lines relevant to our analyses are presented in table 2, though the choice of absolute oscillator strengths is not essential because the analysis of this study is differential relative to the Sun. The observed equivalent widths (which were measured by the method of Gaussian fitting or direct integration depending on cases) and the resulting abundances are given in tables 3 and 4, respectively.

Note that the S abundance from the S I 6052 line was determined by correctly taking into account the blending two components, while the equivalent width was measured as if regarding it as a single line. Also, the non-LTE correction (amounting to ~ 0.1 – 0.4 dex) was taken into consideration for deriving the O abundance from the strong O I 7771, 7774, and 7775 triplet lines according to the calculation of Takeda (2001), as given in the 7th column of table 4.

3.2.2. Spectral synthesis analysis

Meanwhile, refractory element abundances (Si, Ti, V, Fe, Co, and Ni) were determined by the spectrum synthetic technique while applying the automatic fitting algorithm (Takeda 1995), in which the abundances of these 6 elements (along with the macrobroadening parameter and the radial velocity shift) were simultaneously varied to find the best-fit solution such that

minimizing the $O - C$ deviation. This yields accurate and reliable results than the case of conventional analysis. After several trials, the 6080–6089 Å region was found to be adequate (i.e., a satisfactory fit is accomplished with our gf values given in table 2), which we decided to adopt. Note that, apart from those given in table 2, all lines listed in Kurucz and Bell’s (1995) compilation were included as background opacities. The best-fit theoretically synthesized spectra along with the observed spectra are shown in figures 1a and b. Such established abundances are given in table 4.

Similarly, the C and O abundances from [C I] 8727 and O I 6158 lines were obtained by this technique, since these line features are delicately weak and more or less blended with other species. As a result of the analyses of these two line features, the abundances of Si and Fe were simultaneously obtained as by-products. Note that spectral portions, where the line data are so insufficient that the observed spectrum could not be reproduced (e.g., around 6157.3 Å for the case of lower temperature stars), were masked (i.e., excluded from judging the goodness of fit) in the process of automatic fitting. Figures 2 (8727 Å region analysis) and 3 (6157 Å region analysis) show the appearance of the fit, and the resulting abundances are presented in table 4.

3.2.3. Sensitivity to parameter changes

In order to estimate the uncertainties involved with the ambiguities in the atmospheric parameters, we selected v And and 70 Vir as the representatives of higher T_{eff} and lower T_{eff} stars and evaluated the abundance variations in response to changing T_{eff} (by +150 K), $\log g$ (by +0.3), and ξ (by +0.5 km s⁻¹). The results are given in table 5, from which we may state that errors caused by uncertainties in these parameters are not very significant considering the reasonable consistency of the published values (cf. subsection 3.1).

3.2.4. Final results

In table 6, we give the final results of the abundances which will be discussed in section 4.

As for the volatile elements, we adopted a mean value when two or more abundances from different line indicators are available. In this averaging process, a half weight was assigned to the C and O abundance derived from the forbidden lines ([C I] 8727 and [O I] 6300) in view of their comparatively less reliability due to the suspected blending effect, i.e., with unknown species for [C I] (Gonzalez et al. 2001) and with the Ni I line for [O I] (Allende Prieto et al. 2001).

Meanwhile, regarding the refractory elements (Si, Ti, V, Fe, Co, and Ni), we adopted the abundances from the 6080–6089 Å fitting analysis, since we consider the results for these 6 elements from this 6080–6089 Å region is sufficiently accurate.

The T_c values presented in table 6 were taken from Field (1974) for CNO, and from Wasson (1985) for the remaining elements.

4. Discussion

4.1. Fe abundance

The resulting Fe abundances of the program stars (table 6) are compared with the literature values (table 1) in figure 4, where we can see that both are in fairly reasonable agreement. The mean for those 14 stars with planets is $\langle[\text{Fe}/\text{H}]\rangle = +0.12(\pm 0.20)$, which confirms the mild enrichment of metallicity as has been already reported (cf. section 1), though a rather large diversity is observed (e.g., ρ CrB is evidently metal-deficient, though its companion may actually not be a planet as remarked in the footnote to table 1).

4.2. Refractory Elements

Figures 5a–e show the comparison of the abundances of five refractory elements (Si, Ti, V, Co, and Ni) with the Fe abundance. We may state from this figure that the abundances of those elements scale with that of Fe, which is an expected tendency because these belong to the same group in terms of T_c (1300–1500 K).

The reason for the appreciable systematic difference of $[\text{Co}/\text{H}]$ by 0.1–0.2 dex relative to $[\text{Fe}/\text{H}]$ (cf. figure 5d) may be related to the weakness of this line (especially for higher T_{eff} stars; cf. figure 1a), by which the reliability of the results may be more or less lowered.

4.3. Volatile Elements

The results of $[\text{C}/\text{H}]$, $[\text{N}/\text{H}]$, $[\text{O}/\text{H}]$, $[\text{S}/\text{H}]$, and $[\text{Zn}/\text{H}]$ are compared with $[\text{Fe}/\text{H}]$ in figures 6a–e, respectively. These figures suggest that *the abundances of all these five volatile elements scale with that of Fe.*² Especially, the trend of $[\text{C}/\text{Fe}] < 0$ for metal-rich planet-harboring stars, which was once reported before (cf. section 1), can not be confirmed. Hence, our results suggest that the tendency predicted from the “self-enrichment” hypothesis, $[\text{X}/\text{H}] < [\text{Fe}/\text{H}]$ for metal-enriched planet-harboring stars ($[\text{Fe}/\text{H}] > 0$), is not observed at all. (Even a weak inversed trend, $[\text{X}/\text{H}] > [\text{Fe}/\text{H}]$, appears to exist such as for N or S.)

If fractionated solid materials have something to do with any chemical peculiarity in photospheric abundances, some kind of anti-correlation between the abundances of volatile and refractory elements is to be expected. Let us consider, for example, the case of A-type stars (including λ Boo stars). In this class of stars, $[\text{C}/\text{H}]$ is known to be clearly anti-correlated with $[\text{Si}/\text{H}]$, which is suspected as due to the differential accretion of gas and dust in late stages of star formation (see, e.g., Holweger, Stürenburg 1993). On the contrary, in the present case, C and Si behave themselves quite similarly with each other, as shown in figure 7 (compare this figure with their figure 2).

² The trend of appreciable deviation for τ Cet (observed also in figure 5) is (at least partly) attributed to the consequence of the Galactic chemical evolution for α -process elements (e.g., O, S, Si, and Ti), for which metal-deficient stars ($[\text{Fe}/\text{H}] < 0$) are known to show $[\alpha/\text{Fe}] > 0$. However, the reason why this tendency more or less appears in other (non- α) elements is not clear.

We also investigated if there is any systematic trend in $[X/H]$ with respect to T_c , such that reported by Smith et al. (2001) for a subset of planet-harboring stars. We calculated the slope (a) of the linear-regression line ($[X/H]=a \cdot T_c + b$) determined from the $[X/H]$ values of the 11 elements (or 10 elements when N is not available). The results are given in 13th and 14th columns of table 6. By inspecting these a values, the signs of which are randomly positive or negative without showing any systematic dependence with the orbital period/radius of the planets, we may state that the tendency of positive a expected from the self-enrichment hypothesis (cf. section 1) can not be observed.

Consequently, we consider that the “pollution” scenario is rather unlikely for the explanation of the metal-richness of planet-harboring stars, which may lend support for an alternative interpretation that the enhanced metallicity of stars with planets is nothing but a “primordial” characteristics.

5. Conclusion

We determined the abundances of five volatile elements (C, N, O, S, and Zn; low T_c) and six refractory elements (Si, Ti, V, Fe, Co, and Ni; high T_c) for 14 bright planet-bearing stars along with 4 reference stars (+ Sun), based on the spectra obtained by using the high-dispersion echelle spectrograph at Okayama Astrophysical Observatory, in order to examine whether any systematic difference exists between these two groups of elements.

Our results indicate that all of the studied elements behave themselves quite similarly with each other (i.e., $[X/Fe] \simeq 0$) irrespective of whether the element is volatile (apt to be remained in gas phase) or refractory (apt to be included in solid materials). In other words, we could not observe any systematic tendency of $[X/H]$ in terms of T_c .

These facts suggest that the “self-pollution” scenario proposed to explain the enhanced metallicity in planet-harboring stars, which invokes an accretion of metal-rich solid planetesimals (deficient in volatile elements while rich in refractory ones) onto the host star, is rather unlikely, since this mechanism would result in $[X/Fe] < 0$ for $[Fe/H] > 0$ for volatile elements and a systematic increase of $[X/H]$ with T_c .

Therefore, as far as those 14 bright sample stars studied in this investigation are concerned, we would consider that the tendency of metal-richness in planet-bearing stars is of primordial origin (i.e., higher probability of planet formation for intrinsically metal-rich gas) rather than attributing it to an acquired character.

This research have made use of the simbad database, operated at CDS, Strasburg, France. This work is based on observations carried out within the framework of the OAO key project “Comprehensive Spectroscopic Study of Stars with Planets”, which aims to understand the property of planet-harboring stars by analyzing stellar abundances and line-profiles, as well as to improve the precision of measuring stellar radial velocities to a level of planet-detectability.

References

- Allende Prieto, C., Lambert, D. L., & Asplund, M. 2001, *ApJ*, 556, L63
- Arribas, S., & Crivellari, L. 1989, *A&A*, 210, 211
- Drake, J. J., & Smith, G. 1993, *ApJ*, 412, 797
- Feltzing, S., & Gonzalez, G. 2001, *A&A*, 367, 253
- Field, G. B. 1974, *ApJ*, 187, 453
- Fuhrmann, K. 1998, *A&A*, 338, 161
- Gatewood, G., Han, I., & Black, D. C. 2001, *ApJ*, 548, L61
- Gonzalez, G. 1998, *A&A*, 334, 221
- Gonzalez, G., & Laws, C. 2000, *ApJ*, 119, 390
- Gonzalez, G., Laws, C., Tyagi, S., & Reddy, B. E. 2001, *AJ*, 121, 432
- Gonzalez, G., & Vanture, A. D. 1998, *A&A*, 339, L29
- Holweger, H., & Stürenburg 1993, in *ASP Con. Ser. 44, Peculiar Versus Normal Phenomena in A-Type and Related Stars*, ed. M. M. Dworetzky, F. Castelli, & R. Faraggiana (San Francisco: ASP), 356
- Izumiura, H. 1999, in *Proc. 4th East Asian Meeting on Astronomy*, ed. P. S. Chen (Yunnan Observatory, Kunming), 77
- Kurucz, R. L. 1993, *Kurucz CD-ROM, No. 13* (Harvard-Smithsonian Center for Astrophysics)
- Kurucz, R. L., & Bell, B. 1995, *Kurucz CD-ROM, No. 23* (Harvard-Smithsonian Center for Astrophysics) (<http://cfa-www.harvard.edu/amdata/ampdata/kurucz23/>)
- Kurucz, R. L., Furenlid, I., Brault, J., & Testerman, L. 1984, *Solar Flux Atlas from 296 to 1300 nm* (Sunspot, New Mexico: National Solar Observatory)
- Murray, N., & Chaboyer, B. 2001, preprint (astro-ph/0106294)
- Pinsonneault, M. H., DePoy, D. L., & Coffee, M. 2001, *ApJL*, in press (astro-ph/0105257)
- Sadakane, K., Honda, S., Kawanomoto, S., Takeda, Y., & Takada-Hidai, M. 1999, *PASJ*, 51, 501
- Sadakane, K., Ohkubo, M., Sato, S., Osada, K., Takada-Hidai, M., Masuda, S., Izumiura, H., Koyano, H., et al. 2001, *PASJ*, 53, 315
- Santos, N. C., Israelian, G., & Mayor, M. 2000, *A&A*, 363, 228
- Santos, N. C., Israelian, G., & Mayor, M. 2001, *A&A*, submitted (astro-ph/0105216)
- Smith, V. V., Cunha, K., & Lazzaro, D. 2001, *AJ*, in press (astro-ph/0103063)
- Takeda, Y. 1995, *PASJ*, 47, 287
- Takeda, Y. 2001, *ApJ*, submitted (astro-ph/0105215)
- Wasson, J. T. 1985, *Meteorites: The Record of Early Solar System History* (New York: Freeman), appendix G

Table 1. Data and adopted atmospheric parameters of the observed stars.

HD No.	Name	V	Sp	$M \sin i$ (M_J)	a (AU)	P (d)	T_{eff} (K)	$\log g$ (cgs)	[Fe/H]	ξ (km s^{-1})	Reference
120136	τ Boo	4.50	F6IV	3.87	0.05	3.31	6420	4.18	+0.32	1.3	GL
9826	ν And	4.09	F8V	0.71	0.06	4.62	6140	4.12	+0.12	1.4	GL
186427	16 Cyg B	6.20	G2.5V	1.5	1.72	804	5700	4.35	+0.06	1.0	G98
22049	ϵ Eri*	3.73	K2V	0.86	3.3	2502.1	5180	4.75	-0.09	1.3	DS
95128	47 UMa	5.10	G1V	2.4	2.11	1082.02	5800	4.25	+0.01	1.0	G98
89744	HD 89744	5.74	F7V	7.2	0.88	256	6338	4.17	+0.30	1.6	GLTR
217014	51 Peg	5.49	G2.5IVa	0.45	0.05	4.23	5750	4.40	+0.21	1.0	G98
75732	55 Cnc	5.95	G8V	0.84	0.11	14.65	5250	4.40	+0.45	0.8	GV
117176	70 Vir	5.00	G4V	6.6	0.43	116	5500	3.90	-0.03	1.0	G98
143761	ρ CrB [†]	5.40	G0Va	1.1	0.23	39.65	5750	4.10	-0.29	1.2	G98
217107	HD 217107	6.18	G8IV	1.28	0.07	7.13	5600	4.40	+0.36	1.0	GLTR
52265	HD 52265	6.30	G0III-IV	1.13	0.49	118.96	6162	4.29	+0.27	1.2	GLTR
38629	HD 38529	5.94	G4V	0.77	0.13	14.32	5646	3.92	+0.37	1.2	GLTR
145675	14 Her	6.67	K0V	3.3	2.5	1650	5300	4.50	+0.47	1.0	FG
10700	τ Cet	3.50	G8V	5250	4.65	-0.47 [‡]	1.1	AC
61421	α CMi	0.34	F5IV-V	6470	4.01	-0.01	1.9	F98
186408	16 Cyg A	5.96	G1.5V	5750	4.20	+0.11	1.0	G98
102870	β Vir	3.61	F9V	6085	4.04	+0.14	1.4	F98
...	Sun	...	G2V	5780	4.44	0.00	1.0	SHKTT

Note. The V magnitudes and the spectral types are from the SIMBAD database. The data of the mass, the half-major axis, and the period for the planets around planet-harboring stars were taken from the “extrasolar planets” home page (<http://cfa-www.harvard.edu/planets/encycl.html>). The references for the T_{eff} , $\log g$, [Fe/H] and ξ values adopted in this paper are abbreviated in the last column: GL — Gonzalez and Laws (2000), G98 — Gonzalez (1998), DS — Drake and Smith (1993), GLTR — Gonzalez et al. (2001), GV — Gonzalez and Vanture (1998), FG — Feltzing and Gonzalez (2001), AC — Arribas and Crivellari (1989), F98 — Fuhrmann (1998), and SHKTT — Sadakane et al. (1999).

* Chromospherically active star with spectroscopic anomalies (cf. Drake, Smith 1993)

[†] The companion mass may actually not be that of a planet, because its orbital inclination angle (i) is suspected to be very small (i.e., face-on system) according to Gatewood et al. (2001).

[‡] The value from high-excitation Fe I lines was adopted (because of being less affected by a non-LTE effect).

Table 2. Adopted gf values of important lines.*

Species	λ (\AA)	χ (eV)	$\log gf$
C I	5380.34	7.69	-1.84
S I	6052.58	7.87	-1.33
S I	6052.67	7.87	-0.74
V I	6081.44	1.05	-0.58
Co I	6082.42	3.51	-0.52
Fe I	6082.71	2.22	-3.57
Fe II	6084.11	3.20	-3.81
Ti I	6085.23	1.05	-1.35
Fe I	6085.26	2.76	-3.21
Ni I	6086.28	4.27	-0.53
Co I	6086.65	3.41	-1.04
Si I	6087.81	5.87	-1.60
O I	6156.74	10.74	-1.52
O I	6156.76	10.74	-0.93
O I	6156.78	10.74	-0.73
Fe I	6157.73	4.08	-1.26
O I	6158.15	10.74	-1.89
O I	6158.17	10.74	-1.03
O I	6158.19	10.73	-0.44
O I	6300.30	0.00	-9.82
Zn I	6362.34	5.80	+0.15
O I	7771.94	9.15	+0.32
O I	7774.17	9.15	+0.17
O I	7775.39	9.15	-0.05
N I	8683.40	10.33	-0.05
S I	8693.93	7.87	-0.51
S I	8694.63	7.87	+0.08
C I	8727.12	1.26	-8.21
Fe I	8727.13	4.19	-3.93
Si I	8728.01	6.18	-0.61
Si I	8728.59	6.18	-1.72
Fe I	8729.15	3.42	-2.95
Si I	8729.28	6.18	-2.30

* All data were taken from the compilation of Kurucz and Bell (1995).

Table 3. Data of measured equivalent widths (in mÅ).

Star	C5380	S6052	O6300	Zn6362	O7771	O7774	O7775	N8683	S8693	S8694
τ Boo	56.8	35.9	...	29.6	158.8	138.2	125.2	36.2	52.0	85.1
ν And	41.5	25.1	4.6	24.5	122.9	115.8	96.4	19.6	29.1	55.1
16 Cyg B	23.9	11.2	6.5	18.8	70.3	60.7	54.4	10.8	11.8	30.8
ϵ Eri	9.8	5.5	5.2	9.3
47 UMa	25.8	13.8	6.0	22.8	82.8	79.5	60.6	13.0	13.8	33.2
HD 89744	43.0	28.5	4.9	26.9	137.3	131.0	111.3	22.9	29.9	63.7
51 Peg	29.5	18.2	7.2	25.4
55 Cnc	19.5	20.1	9.9	26.6	45.2	49.9	31.1	10.5	9.0	20.3
70 Vir	14.9	10.4	9.5	19.3	62.9	54.9	42.2	4.0	13.3	19.5
ρ CrB	15.9	10.8	5.4	19.1	72.8	73.0	56.4	6.1	11.4	27.8
HD 217107	29.4	23.6	8.7	26.8
HD 52265	37.1	25.5	7.4	26.1	118.8	111.3	88.0	16.6	27.4	54.3
HD 38529	35.5	27.0	12.5	36.2	85.5	82.8	63.7	17.0	30.5	42.0
14 Her	23.9	23.7	8.4	29.2
τ Cet	6.7	4.8	5.0	10.7
α CMi	51.6	24.9	3.6	15.9	170.4	164.1	136.5	30.2	28.7	59.3
16 Cyg A	24.6	15.3	7.4	24.4	79.6	66.5	59.4	8.0	16.0	32.5
β Vir	38.7	22.8	6.6	26.3
Sun	19.9	11.2	5.2	19.7	72.4	62.7	47.9	6.4	10.6	27.3

Table 4. Comparison of the abundances from different lines.

Star	[C] ₅₃₈₀	[C] ₈₇₂₇ ^{fit}	[O] ₆₁₅₈ ^{fit}	[O] ₆₃₀₀	[O] ₇₇₇₃	Δ_{7773}	[Si] ₆₀₈₇ ^{fit}	[Si] ₈₇₂₈ ^{fit}	[S] ₆₀₅₂	[S] ₈₆₉₄	[Fe] ₆₀₈₅ ^{fit}	[Fe] ₆₁₅₇ ^{fit}	[Fe] ₈₇₂₉ ^{fit}
τ Boo	+0.31	+0.42	+0.09	...	+0.19	(-0.38)	+0.26	+0.38	+0.28	+0.59	+0.18	+0.21	+0.27
ν And	+0.19	+0.29	+0.07	-0.08	+0.14	(-0.27)	+0.18	+0.24	+0.16	+0.28	+0.10	+0.09	+0.11
16 Cyg B	+0.13	-0.02	+0.06	+0.07	+0.07	(-0.11)	+0.09	+0.10	+0.02	+0.08	+0.05	+0.05	+0.09
ϵ Eri	+0.14	+0.00	-0.04	...	+0.17	...	-0.10
47 UMa	+0.10	+0.05	+0.05	-0.01	+0.11	(-0.15)	+0.01	+0.05	+0.04	+0.08	-0.08	-0.05	-0.01
HD 89744	+0.13	+0.34	+0.02	+0.07	+0.10	(-0.31)	+0.26	+0.27	+0.16	+0.21	+0.21	+0.15	+0.35
51 Peg	+0.26	...	+0.20	+0.20	+0.16	...	+0.26	...	+0.19	+0.21	...
55 Cnc	+0.33	-0.34	...	+0.37	+0.29	(-0.06)	+0.26	+0.50	+0.69	+0.33	+0.27	...	+0.43
70 Vir	-0.17	-0.11	-0.07	-0.01	-0.02	(-0.13)	-0.01	-0.02	-0.04	+0.15	-0.08	-0.06	-0.08
ρ CrB	-0.19	-0.25	+0.08	-0.23	-0.02	(-0.15)	-0.13	-0.17	-0.09	-0.05	-0.30	-0.29	-0.24
HD 217107	+0.36	...	+0.27	+0.32	+0.27	...	+0.52	...	+0.28	+0.26	...
HD 52265	+0.15	+0.33	+0.09	+0.26	+0.14	(-0.24)	+0.24	+0.43	+0.21	+0.28	+0.19	+0.26	+0.27
HD 38529	+0.31	+0.25	+0.23	+0.30	+0.19	(-0.19)	+0.35	+0.37	+0.42	+0.60	+0.37	+0.41	+0.39
14 Her	+0.46	+0.35	+0.36	...	+0.79	...	+0.39
τ Cet	-0.13	-0.18	-0.21	...	+0.03	...	-0.58
α CMi	+0.15	+0.26	+0.07	-0.16	+0.17	(-0.43)	-0.05	+0.04	+0.00	+0.07	-0.08	-0.17	+0.07
16 Cyg A	+0.06	-0.38	+0.04	+0.09	+0.06	(-0.14)	+0.09	+0.12	+0.10	+0.18	+0.07	+0.12	+0.10
β Vir	+0.14	...	+0.10	+0.04	+0.16	...	+0.11	...	+0.11
Sun	8.67	8.41	8.87	8.97	8.83	(-0.11)	7.46	7.84	7.36	7.19	7.54	7.62	7.64

Note. The presented stellar abundances are the differential ones ($[X] \equiv \log \epsilon_X - \log \epsilon_{\odot}$) relative to the solar abundance given in the last row ($\log \epsilon_{\odot}$; expressed with the usual normalization of $\log \epsilon_{\text{H}} = 12.00$). The values in the 7th column are the non-LTE corrections ($\Delta \equiv \log \epsilon_{\text{NLTE}} - \log \epsilon_{\text{LTE}}$) for the O I 7771-5 triplet (mean of the three lines) showing an appreciable non-LTE effect, while LTE was assumed for the other two oxygen lines (O I 6158 and [O I] 6300) for which this correction is negligibly small (cf. Takeda 2001).

Table 5. Abundance variations to changes in the model parameters.

	Δ_T^*	Δ_g^\dagger	Δ_ξ^\ddagger	Δ_T^*	Δ_g^\dagger	Δ_ξ^\ddagger
	<i>v</i> And			70 Vir		
	(6140 K, 4.12, 1.4 km s ⁻¹)			(5500 K, 3.90, 1.0 km s ⁻¹)		
(Analysis of individual lines)						
C I 5380	-0.07	+0.09	-0.02	-0.09	+0.10	+0.00
N I 8683	-0.11	+0.10	+0.01	-0.13	+0.10	+0.02
O I 6300	+0.04	+0.12	+0.00	+0.03	+0.13	+0.00
O I 7771	-0.11	+0.05	-0.08	-0.16	+0.08	-0.05
O I 7774	-0.12	+0.05	-0.08	-0.16	+0.09	-0.05
O I 7775	-0.11	+0.07	-0.07	-0.15	+0.10	-0.04
S I 6052	-0.06	+0.08	-0.01	-0.09	+0.10	+0.00
S I 8693	-0.08	+0.08	-0.02	-0.11	+0.10	-0.01
S I 8694	-0.08	+0.07	-0.04	-0.11	+0.09	-0.02
Zn I 6362	+0.03	+0.04	-0.03	-0.03	+0.07	-0.03
(6080–6089 Å fitting analysis)						
Si	+0.06	+0.01	+0.00	+0.03	+0.05	+0.00
Ti	+0.23	-0.11	+0.00	+0.22	-0.04	-0.05
V	+0.11	+0.00	-0.01	+0.16	-0.01	-0.03
Fe	+0.05	+0.06	-0.04	+0.08	+0.04	-0.07
Co	+0.15	-0.06	+0.00	+0.10	+0.02	-0.02
Ni	+0.08	+0.00	-0.06	+0.07	+0.03	-0.09
(6156.5–6158.5 Å fitting analysis)						
O	-0.12	+0.11	+0.00	-0.14	+0.10	-0.01
Fe	+0.09	-0.01	-0.11	+0.10	+0.00	-0.19
(8726–8730.5 Å fitting analysis)						
C	+0.01	+0.11	+0.00	-0.05	+0.15	-0.01
Si	+0.04	-0.03	-0.07	-0.01	+0.01	-0.07
Fe	+0.09	+0.01	+0.02	+0.11	+0.00	-0.03

* $\Delta T_{\text{eff}} = +150$ K.† $\Delta \log g = +0.3$.‡ $\Delta \xi = +0.5$ km s⁻¹.

Table 6. Final results of the abundances.

T_c (K)	[C]	[N]	[O]	[S]	[Zn]	[Si]	[Fe]	[Co]	[Ni]	[V]	[Ti]	Slope a^*	
	75	120	180	648	660	1311	1336	1351	1354	1450	1549	with N	without N
	Volatile elements					Refractory elements							
τ Boo	+0.35	+0.47	+0.14	+0.44	+0.29	+0.26	+0.18	+0.42	+0.24	+0.10	+0.22	-8.45	-4.58
v And	+0.22	+0.24	+0.07	+0.22	+0.07	+0.18	+0.10	+0.26	+0.12	+0.14	+0.08	-2.78	-0.76
16 Cyg B	+0.08	+0.31	+0.07	+0.05	-0.02	+0.09	+0.05	+0.12	+0.10	+0.07	+0.00	-5.19	+0.74
ϵ Eri	+0.14	...	+0.00	+0.17	-0.15	-0.04	-0.10	+0.00	-0.13	+0.08	-0.05	...	-8.16
47 UMa	+0.08	+0.31	+0.06	+0.06	+0.06	+0.01	-0.08	-0.01	-0.04	-0.05	-0.11	-15.81	-10.77
HD 89744	+0.20	+0.19	+0.06	+0.19	+0.17	+0.26	+0.21	+0.38	+0.16	+0.27	+0.24	+7.99	+9.32
51 Peg	+0.26	...	+0.20	+0.26	+0.20	+0.16	+0.19	+0.30	+0.29	+0.12	+0.12	...	-3.83
55 Cnc	+0.11	+0.71	+0.32	+0.51	+0.51	+0.26	+0.27	+0.55	+0.50	+0.46	+0.18	-3.06	+6.15
70 Vir	-0.15	-0.17	-0.04	+0.05	-0.08	-0.01	-0.08	+0.02	-0.09	-0.05	-0.10	+3.93	+1.50
ρ CrB	-0.21	-0.05	-0.02	-0.07	-0.13	-0.13	-0.30	-0.15	-0.30	-0.21	-0.18	-9.42	-8.32
HD 217107	+0.36	...	+0.29	+0.52	+0.31	+0.27	+0.28	+0.49	+0.41	+0.33	+0.20	...	-2.69
HD 52265	+0.21	+0.15	+0.14	+0.25	+0.17	+0.24	+0.19	+0.39	+0.25	+0.26	+0.28	+7.85	+7.28
HD 38529	+0.29	+0.46	+0.23	+0.51	+0.39	+0.35	+0.37	+0.58	+0.45	+0.48	+0.31	+5.79	+9.12
14 Her	+0.46	...	+0.35	+0.79	+0.56	+0.36	+0.39	+0.67	+0.59	+0.58	+0.35	...	+0.11
τ Cet	-0.13	...	-0.18	+0.03	-0.21	-0.21	-0.58	-0.33	-0.51	-0.43	-0.45	...	-25.44
α CMi	+0.19	+0.27	+0.06	+0.03	-0.12	-0.05	-0.08	+0.10	-0.13	-0.07	-0.25	-19.31	-15.45
16 Cyg A	-0.09	+0.04	+0.06	+0.14	+0.11	+0.09	+0.07	+0.16	+0.14	+0.12	+0.09	+7.40	+7.85
β Vir	+0.14	...	+0.08	+0.11	+0.10	+0.16	+0.11	+0.22	+0.13	+0.09	+0.10	...	+1.77
Sun	8.58	8.13	8.87	7.28	4.51	7.46	7.54	4.72	6.35	3.89	5.01	—	—

Note. The abundance results presented here are the differential values relative to the solar abundances (given in the last row).

* The slope (a ; expressed in unit of 10^{-5} dex K^{-1}) of the linear-regression line, $[X/H]=a \cdot T_c + b$.

Fig.1a

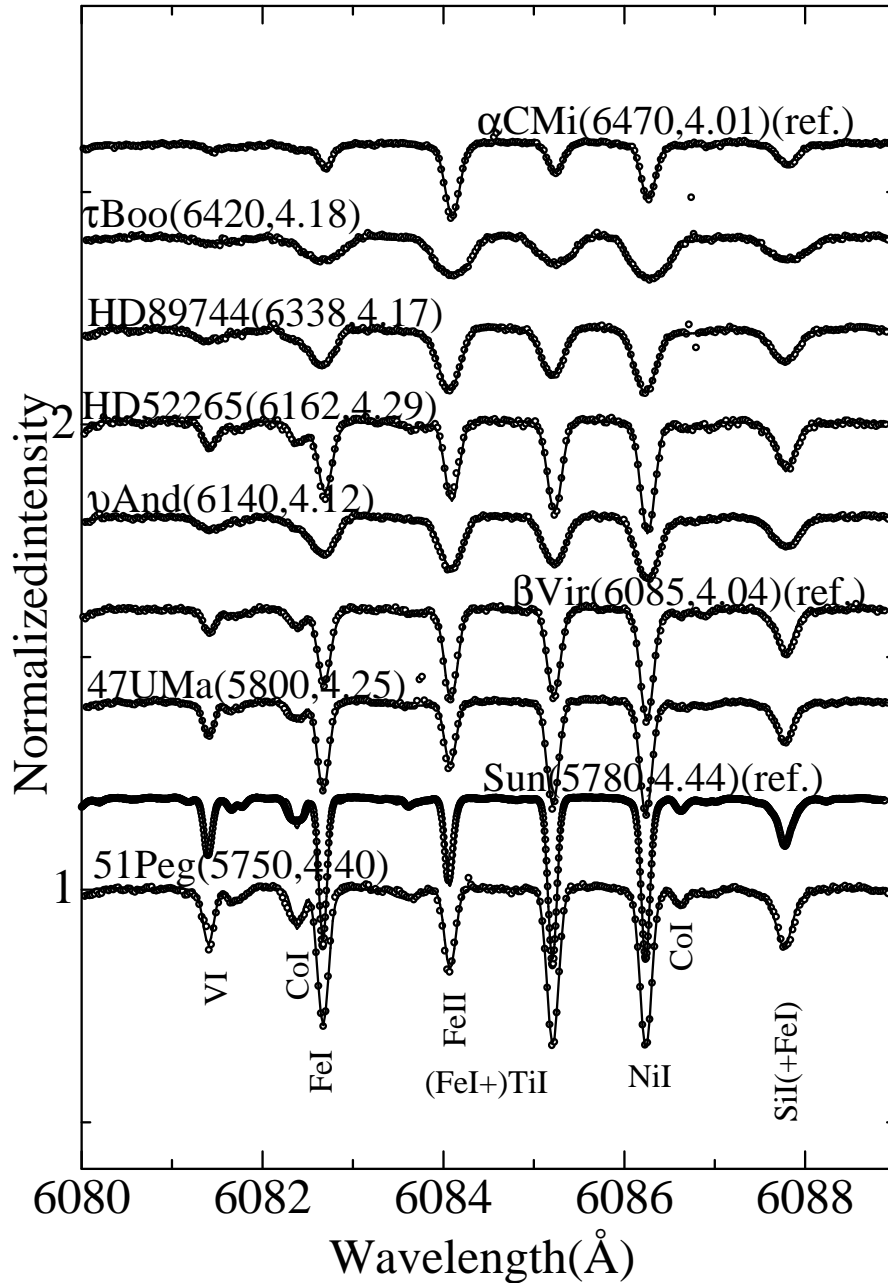


Fig. 1. Spectral fitting at the 6080–6089 Å region to determine the abundances of Si, Ti, V, Fe, Co, and Ni. Open circles denote the observed data, while the solid curves represent the best-fit theoretical spectra. Each of the spectra, arranged in the decreasing order of T_{eff} , are vertically offset by 0.2 with respect to the adjacent one.

(a) Higher T_{eff} stars with $5750 \text{ K} \lesssim T_{\text{eff}} \lesssim 6500 \text{ K}$.

Fig.1b

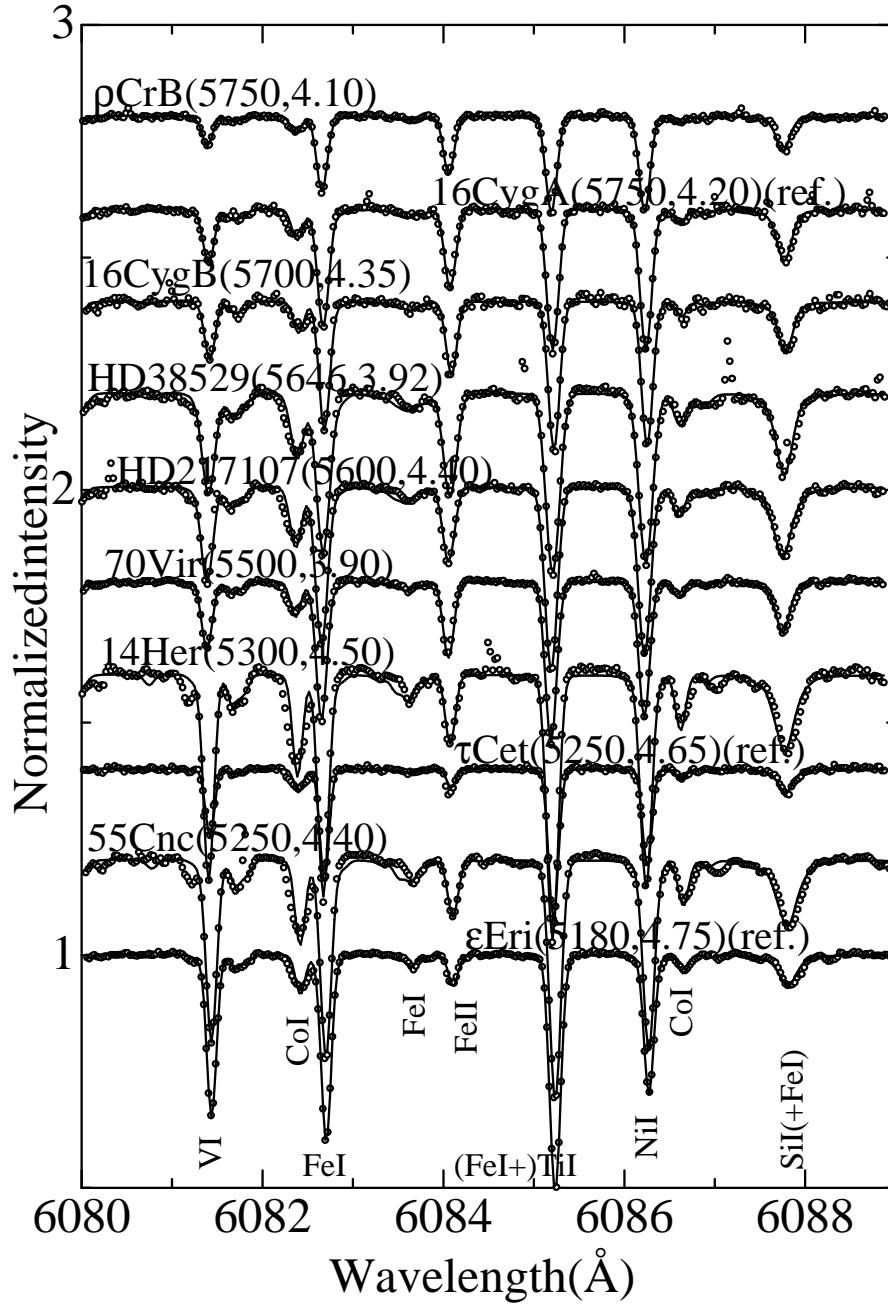


Fig. 1. (b) Lower T_{eff} stars with $5200 \text{ K} \lesssim T_{\text{eff}} \lesssim 5750 \text{ K}$.

Fig.2

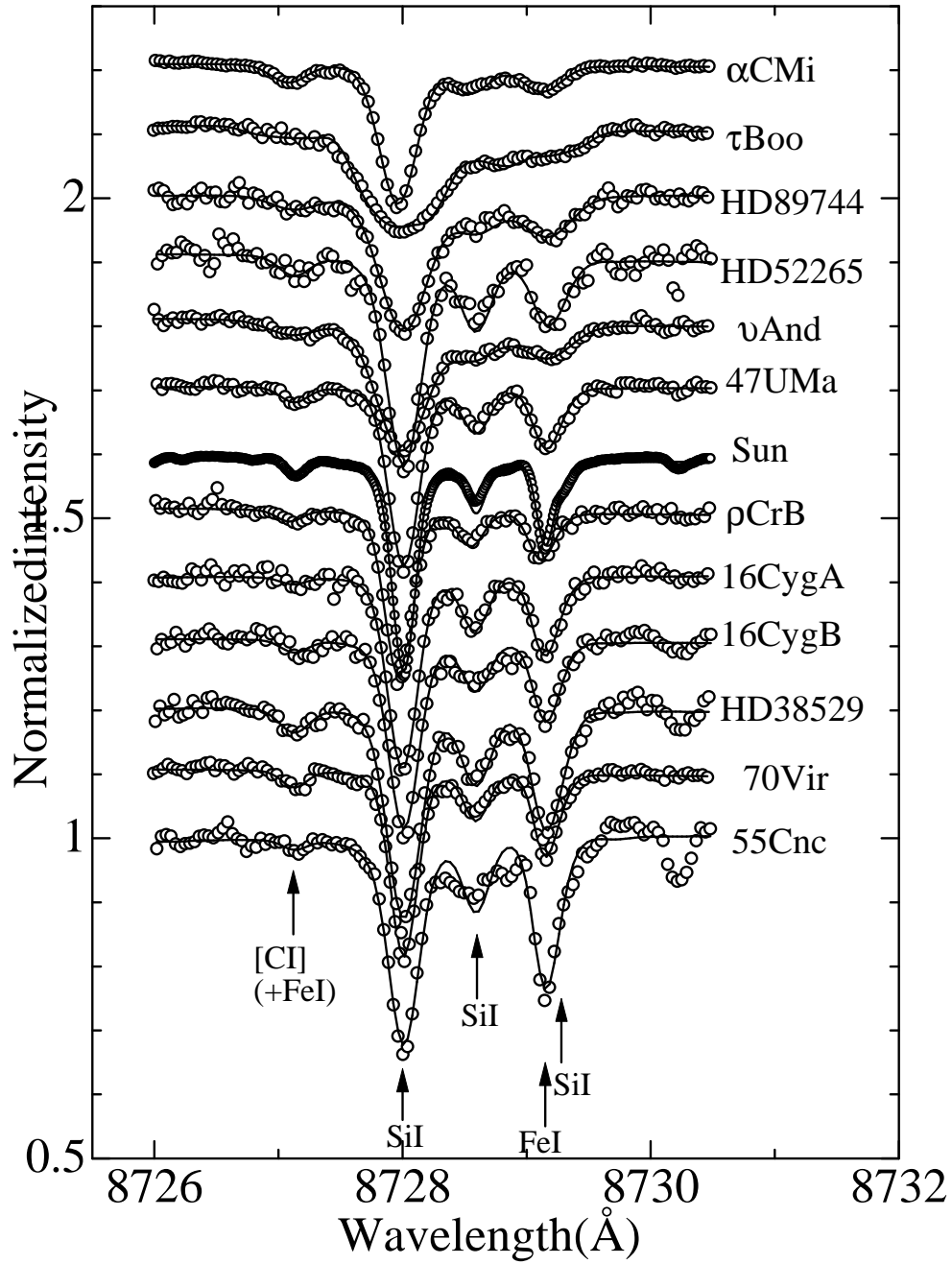


Fig. 2. Spectra fitting at the 8726–8730.5 Å region to determine the abundances of C, Si, and Fe. A vertical offset of 0.1 is applied to each spectra relative to the adjacent one. Otherwise, the same as in figure 1.

Fig.3

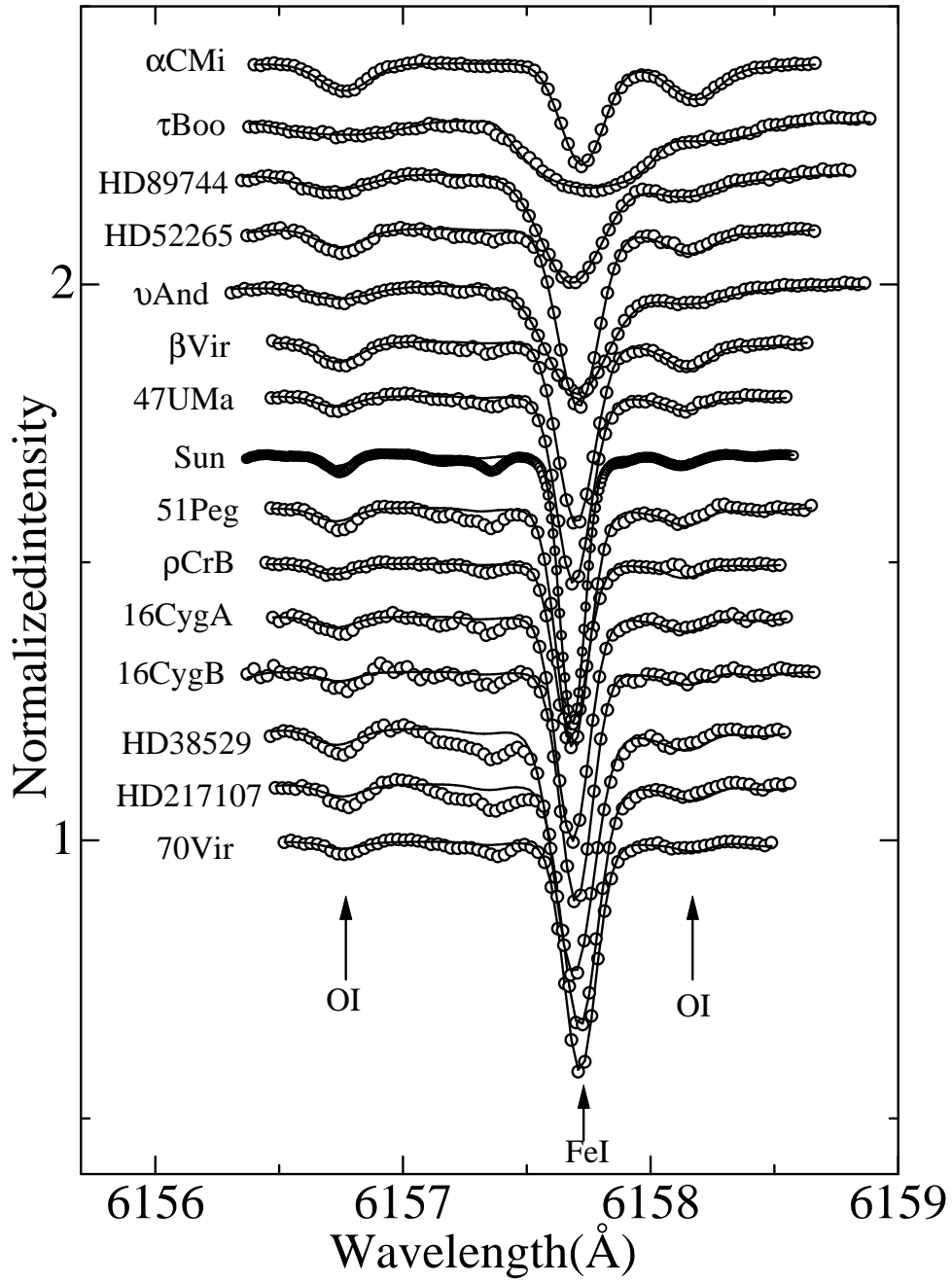


Fig. 3. Spectra fitting at the 6156.5–6158.5 Å region to determine the abundances of O and Fe. A vertical offset of 0.1 is applied to each spectra relative to the adjacent one. Otherwise, the same as in figure 1.

Fig.4

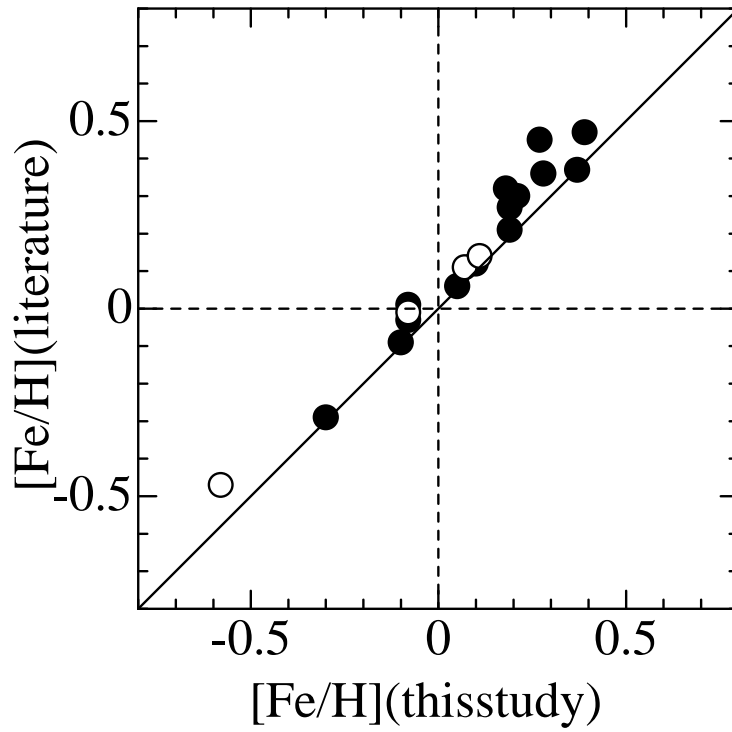


Fig. 4. Comparison of the [Fe/H] values derived in this study with those taken from various literatures (cf. table 1). Filled circles correspond to planet-harboring stars, while open circles to the reference stars.

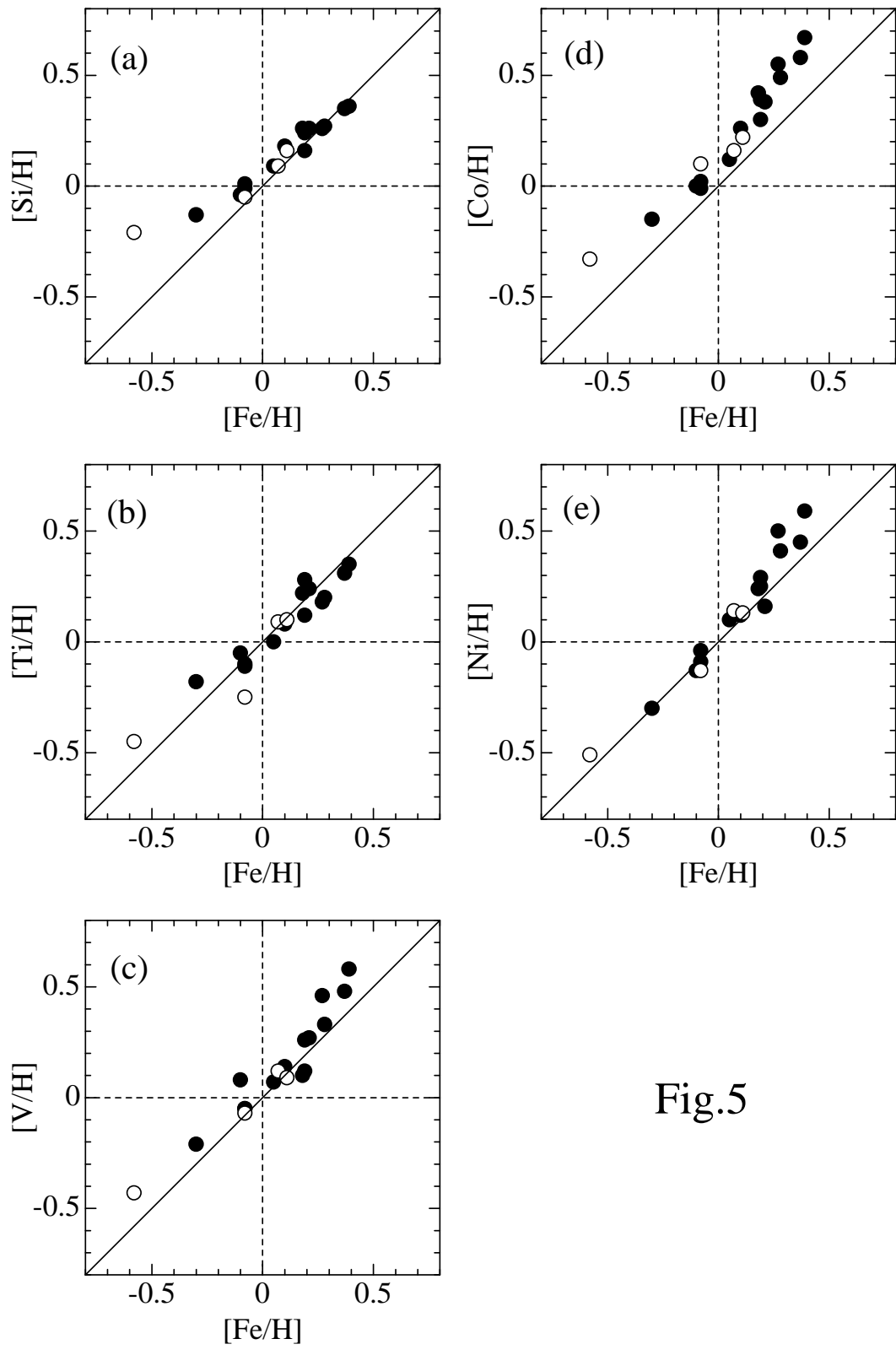


Fig.5

Fig. 5. Comparison of the abundances of five refractory elements with the Fe abundance: (a) Si, (b) Ti, (c) V, (d) Co, and (e) Ni. The same meanings of the symbols as in figure 4.

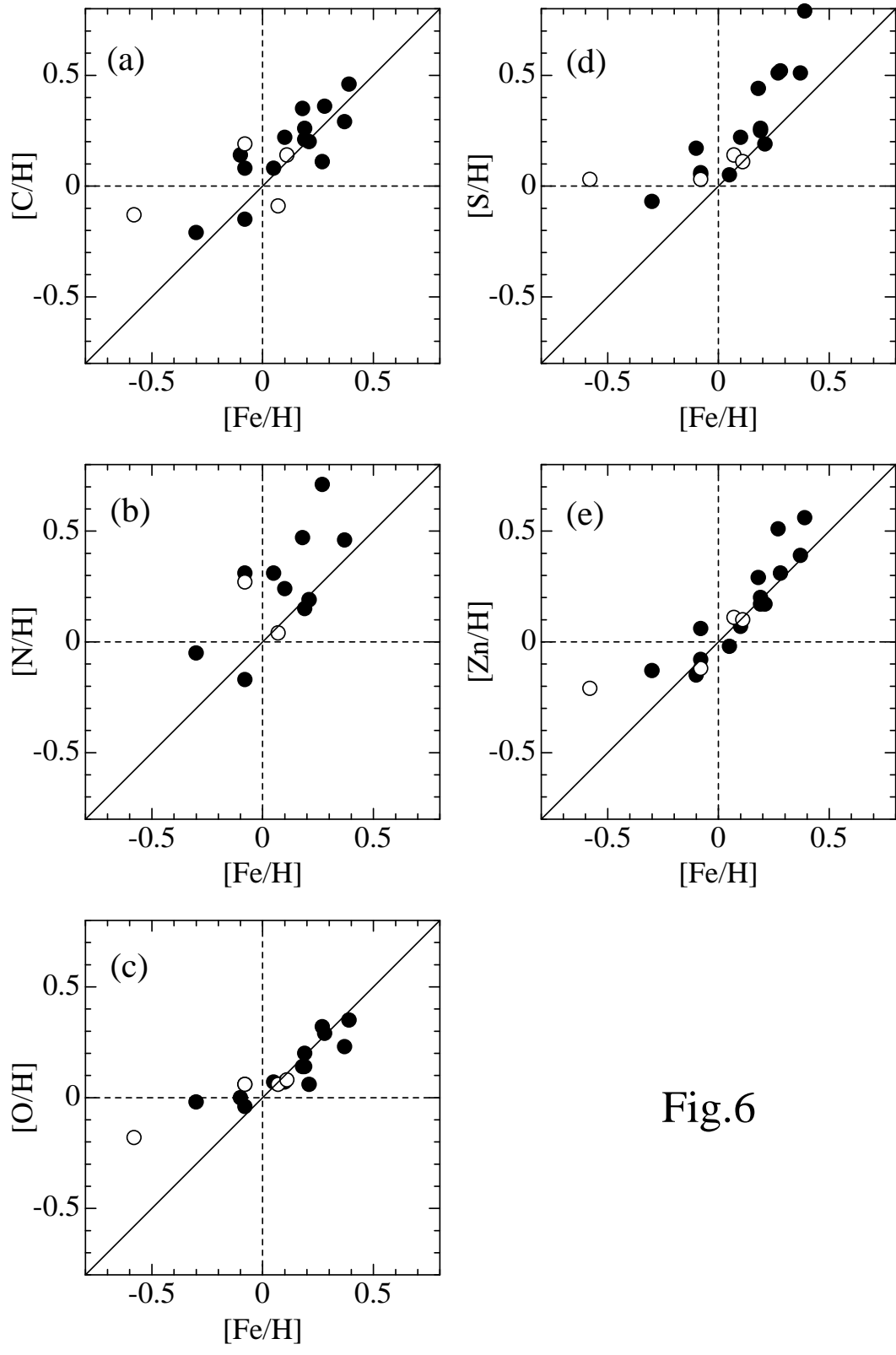


Fig.6

Fig. 6. Comparison of the abundances of five volatile elements with the Fe abundance: (a) C, (b) N, (c) O, (d) S, and (e) Zn. The same meanings of the symbols as in figure 4.

Fig.7

